Modelling of surface segregation for palladium alloys in vacuum and gas environments

Zhao, Meng; Sloof, Willem G.; Bottger, Amarante

DOI
10.1016/j.ijhydene.2017.12.039

Publication date
2018

Document Version
Accepted author manuscript

Published in
International Journal of Hydrogen Energy

Link to formal publication "International Journal of Hydrogen Energy" (Elsevier): https://doi.org/10.1016/j.ijhydene.2017.12.039

Modelling of Surface Segregation for Palladium Alloys in Vacuum and Gas Environments

Meng Zhao, Willem G. Sloof, Amarante J. Böttger*

Department of Materials Science and Engineering, Delft University of Technology, Mekelweg 2, 2628 CD Delft, The Netherlands

Abstract

Surface segregation of a series of forty Palladium-based binary alloys has been investigated using a thermodynamic model based on an atom exchange approach. Their surface segregation behaviour, both in vacuum and in gas environments, were comprehensively estimated. The calculated results are in good agreement with the available experimental and computational data reported in literatures. Effects of mixing enthalpy, temperature, crystal orientation on the surface, elastic strain energy, adsorption and absorption of gases like H_2, O_2, CO have been discussed in detail. These results can be considered as basic guidelines to design novel Pd alloys for hydrogen separation membranes, sensors or catalysts. The model itself also offers a convenient and accurate routine to predict the surface segregation of other than Pd-based binary alloys in different gas atmospheres.

Key words: surface segregation; thermodynamic modelling; Palladium alloy; hydrogen separation

Corresponding author: Amarante J. Bottger

Email: A.J. Bottger@tudelft.nl

1. Introduction

Surface segregation of binary alloys, *i.e.* the surface enrichment by one of the alloy elements, is of great importance as it may enhance or suppress desirable and undesirable chemical reactions at the surface [1]. This phenomenon has been intensively investigated over decades since it became well known that catalytic activity of alloy catalysts is determined almost exclusively by the surface properties [2]. There have been numerous theoretical and experimental efforts made to estimate the surface segregation of various alloys [3, 4]. In particular, Palladium binary alloys were studied, because of their application as storage, catalysts and membrane reactor for hydrogen separation, key components towards the hydrogen economy [5-7].

Currently, about 80% of the world energy demand comes from fossil fuels [8]. Use of hydrogen as an alternative energy source could help to address environmental issues [9]. Besides, hydrogen also has many other applications in various industrial aspects, such as petroleum refining, semiconductor manufacturing, pharmaceuticals etc. [10, 11]. Therefore, the demand for hydrogen has grown for decades, which has motivated improving production methods. Hydrogen can be produced from water by electrolysis, but the most economical method is steam methane reforming (SMR) [12]. The composition of the SMR product stream is typically 74% H_2, 18% CO_2, 7% CH_4 and 1% CO [13]. However, a majority of hydrogen applications require a minimum purity of 99.99%, while polymer-electrolyte fuel cells (PEFCs) require even ultra-pure hydrogen (99.9995%) [14, 15]. Thus, hydrogen separation and purification are essential processes in the hydrogen industry [16, 17].

Palladium (Pd) membranes offer an efficient method for separating hydrogen from a hot gas mixture to high purity levels because of their great hydrogen permeability and selectivity [6, 13, 18]. To improve the performance and lifetime of the membrane, Pd is usually alloyed with transition metals [19, 20]. Alloying can prevent hydrogen embrittlement of Pd by

suppressing hydride formation that is accompanied with a large volume change. Also, alloying may improve the hydrogen permeability and in some cases enhance the resistance to contamination by sulphur containing impurities [21]. At present, most of commercial hydrogen separation membranes are based on Pd-Ag or Pd-Cu alloys [22, 23]. However, surface segregation is a major problem that arise when Pd alloy membranes are kept in a hydrogen environment [24, 25]. Driving forces for surface segregation may be different depending on the conditions: the gas environment, temperature, enthalpies of mixing, surface energy, size mismatch of the atoms and the entropy contribution are only some of the parameters that influence the segregation process. A comprehensive understanding of surface segregation is of paramount importance for further improvement of Pd alloys for membranes, catalysts or sensors.

Thermodynamic calculation provides a cheap and fast way to predict the surface segregation in vacuum and gas environments without the need of expensive and time-consuming experiments. Models on surface segregation in vacuum have been developed since 1950s. For example, Wynblatt and Ku proposed a thermodynamic model to describe the surface segregation in vacuum, with the surface energy reduction as the major driving force [26]. The enthalpy change was accounted for by an "atom exchange approach": an atom located in the bulk, exchanges position with an atom of the other species located at the surface. As for the influence of adsorption or chemisorption, Tomanek determined the surface segregation for H, O and CO covered surfaces by adding the adsorption enthalpy to the total driving force of segregation, and the effect of absorption (of hydrogen) in the bulk was accounted for by using an empirical parameter [27]. However, this is not a universal method to account for gas absorption (of hydrogen) for various Pd alloys or other alloy systems. There are also some other simulation methods dealing with surface segregation phenomena. For example, Monte Carlo simulations have been applied to predict the surface segregation of

binary alloys in vacuum [28]. Density functional theory can also be used to account for the gas adsorption for some specific alloys [29]. However, all these approaches reported do not consider the effect of both gas adsorption and absorption at the same time as would be the case for Pd-based alloys under application conditions.

In the present research, a thermodynamic model also based on the atom exchange approach was developed to describe the surface segregation of a series of forty Pd-based binary alloys. A relation between the surface and bulk compositions upon segregation was obtained for the cases of binary alloys in vacuum, with adsorption on the surface, with absorption in the bulk, and both adsorption and absorption. Effect of hydrogen absorption was considered by the formation enthalpy of metal hydride, which is also feasible for other alloy systems. For a limited set of Pd-binary alloys (Pd-Ag, Pd-Au, Pd-Cu, Pd-Ni and Pd-Pt alloys), experimental and computational results are reported. Those results were compared with our results and a good agreement was obtained.

2. Method

2.1 Surface segregation by atom exchange

Surface segregation refers to the difference in concentration between the surface and the bulk of a material, *i.e.* the surface is enriched with one or several of the constituents. Here surface is defined specifically as the topmost atomic layer only. As mentioned above, surface energy, enthalpy of mixing and elastic strain energy are only some of the aspects contributing to the driving force of the segregation process. Four different cases are considered in the present work, surface segregation (1) in vacuum; (2) with hydrogen adsorption at the surface; (3) with hydrogen absorption in the bulk and (4) with both hydrogen adsorption and absorption, as illustrated in Fig.1.

In case (1), surface segregation in vacuum will be considered using the basic assumption as Wynblatt and Ku's work [26]. The enthalpy of segregation is then related to the change in the

configurational energies of A and B atoms upon their exchange between the bulk and surface, as well as the related elastic strain energy. The segregation enthalpy ΔH_{seg} consist of the change of configurational energy change and the elastic strain energy, $\Delta H_{\text{seg}} = \Delta E_{\text{conf}} + \Delta E_{\text{elastic}}$. ΔE_{conf} can be expressed as [26]:

$$\Delta E_{\text{conf}} = \left(\gamma_{\text{A}}\sigma_{\text{A}} - \gamma_{\text{B}}\sigma_{\text{B}}\right) + 2\omega Z_l \left(x_{\text{A}}^{\text{bulk}} - x_{\text{A}}^{\text{surf}}\right) + 2\omega Z_v \left(x_{\text{A}}^{\text{bulk}} - \frac{1}{2}\right) \quad (1)$$

where γ_{A} and γ_{B} are surface energy of pure A and B metals; σ_{A} and σ_{B} are surface area of A and B directly related to the atomic volume; $x_{\text{A}}^{\text{bulk}}$ and $x_{\text{A}}^{\text{surf}}$ are the solute composition in the bulk material and on the surface. Z_l and Z_v are numbers of nearest lateral and vertical neighbours. For Pd-based alloys with FCC structure, Z_l=6 and Z_v=3 in the (111) plane, while Z_l=Z_v=4 in the (100) plane.

The alloy parameter ω, indicates whether the A-A or B-B bonds are preferred (ω>0, A-A and B-B bonds preferred, and ω<0, A-B bonds preferred) [30]:

$$\omega = \varepsilon_{\text{AB}} - \left(\frac{\varepsilon_{\text{AA}} + \varepsilon_{\text{BB}}}{2}\right) \quad (2)$$

The value of ω of binary alloys can be calculated by the Macroscopic atom model, also called Miedema's model (section 2.2).

The elastic strain energy contribution to the total segregation enthalpy ($\Delta H_{\text{seg}} = \Delta E_{\text{conf}} + \Delta E_{\text{elastic}}$) for isotropic polycrystalline metals A and B is given by [31]:

$$\Delta E_{\text{elastic}} = \frac{2K_{\text{A}}G_{\text{B}}\left(V_{\text{A}} - V_{\text{B}}\right)^2}{3K_{\text{A}}V_{\text{B}} + 4G_{\text{B}}V_{\text{A}}} \quad (3)$$

where V is the atomic volume, K and G represent the bulk modulus and shear modulus. The subscripts A and B correspond to the solute and solvent element, respectively.

Eq.1-3 describe the segregation enthalpy of binary alloys in vacuum. This model offers the possibility to add the enthalpy contribution for adsorbed gas molecules or atoms in the case of dissociative adsorption.

In case (2): for hydrogen adsorption on the surface, the adsorption enthalpy needs to be added [17]. Then the change of segregation enthalpy with hydrogen adsorption is:

$$\Delta E_{\mathrm{conf}}^{\mathrm{ad}} = \left(\gamma_{\mathrm{A}}\sigma_{\mathrm{A}} - \gamma_{\mathrm{B}}\sigma_{\mathrm{B}}\right) + 2\omega Z_l\left(x_{\mathrm{A}}^{\mathrm{bulk}} - x_{\mathrm{A}}^{\mathrm{surf}}\right) + 2\omega Z_v\left(x_{\mathrm{A}}^{\mathrm{bulk}} - \frac{1}{2}\right) + \theta\left(\varepsilon_{\mathrm{AH}} - \varepsilon_{\mathrm{BH}}\right) \quad (4)$$

Here, θ is the adsorbate coverage, where θ=1 means a monolayer adsorption. $\varepsilon_{\mathrm{AH}}$ and $\varepsilon_{\mathrm{BH}}$ are the hydrogen adsorption energy on A and B. Similarly, other adsorbed gases like O, CO and other impurity gases can be added.

In case (3): when hydrogen is absorbed in the bulk of alloys, instead of Tomanek's empirical approach, the solution enthalpy of hydrogen in a metal is estimated through Miedema's model (section 2.2). The segregation enthalpy becomes:

$$\Delta E_{\mathrm{conf}}^{\mathrm{ab}} = \left(\gamma_{\mathrm{A}}\sigma_{\mathrm{A}} - \gamma_{\mathrm{B}}\sigma_{\mathrm{B}}\right) + 2\omega Z_l\left(x_{\mathrm{A}}^{\mathrm{bulk}} - x_{\mathrm{A}}^{\mathrm{surf}}\right) + 2\omega Z_v\left(x_{\mathrm{A}}^{\mathrm{bulk}} - \frac{1}{2}\right) + Z_v x_{\mathrm{H}}\left(\Delta H_{\mathrm{HinB}}^{\mathrm{sol}} - \Delta H_{\mathrm{HinA}}^{\mathrm{sol}}\right) \quad (5)$$

where x_{H} is the amount of absorbed H in the bulk, expressed as the number of H atoms per metal atom (H/M). $\Delta H_{\mathrm{HinA}}^{\mathrm{sol}}$ and $\Delta H_{\mathrm{HinB}}^{\mathrm{sol}}$ are the enthalpies of solution of hydrogen in A and B.

In case (4): with both hydrogen adsorption and absorption, the change of segregation enthalpy is simply defined by a combination of Eq. 4 and 5:

$$\begin{aligned}\Delta E_{\mathrm{conf}}^{\mathrm{ad+ab}} = {} & \left(\gamma_{\mathrm{A}}\sigma_{\mathrm{A}} - \gamma_{\mathrm{B}}\sigma_{\mathrm{B}}\right) + 2\omega Z_l\left(x_{\mathrm{A}}^{\mathrm{bulk}} - x_{\mathrm{A}}^{\mathrm{surf}}\right) + 2\omega Z_v\left(x_{\mathrm{A}}^{\mathrm{bulk}} - \frac{1}{2}\right) + \theta\left(\varepsilon_{\mathrm{AH}} - \varepsilon_{\mathrm{BH}}\right) \\ & + Z_{\mathrm{v}} x_{\mathrm{H}}\left(\Delta H_{\mathrm{HinA}}^{\mathrm{sol}} - \Delta H_{\mathrm{HinB}}^{\mathrm{sol}}\right)\end{aligned} \quad (6)$$

2.2 Miedema's model for mixing enthalpy

A key point of calculating the segregation enthalpy is to define the value of ω, which is directly related to ΔH_{mix}, the mixing enthalpy of binary alloys. For a regular solid solution, ω is defined as [32]:

$$\omega = \frac{\Delta H_{\mathrm{mix}}}{Z x_{\mathrm{A}} \left(1 - x_{\mathrm{A}}\right)} \quad (7)$$

where $Z=Z_l+2Z_v$ is the total number of nearest neighbours and x_{A} is the solute concentration expressed in atom fraction.

To obtain the mixing enthalpy of binary alloys, Miedema's model was used as it has been reported to be successful for many binary alloys [33]. In this model, the alloys are considered to be built of atomic cells of two elements with defined atomic volume. The mixing enthalpy, equal to the formation enthalpy, can then be calculated as:

$$\Delta H_{\mathrm{mix}} = \Delta H_{\mathrm{AinB}}^{\mathrm{formation}} = c_{\mathrm{A}} f_{\mathrm{B}}^{\mathrm{A}} \Delta H_{\mathrm{AinB}}^{\mathrm{sol}} \quad (8)$$

where c_{A} is the solute fraction. $f_{\mathrm{B}}^{\mathrm{A}}$ is a parameter representing the degree to which an atomic cell of A is surrounded by B atoms. For example, $f_{\mathrm{B}}^{\mathrm{A}} = 1$ means A is fully surrounded by B. $f_{\mathrm{B}}^{\mathrm{A}}$ is evaluated by:

$$f_{\mathrm{B}}^{\mathrm{A}} = \left(1 - c_{\mathrm{A}}^{\mathrm{S}}\right)\left[1 + 8\left(c_{\mathrm{A}}^{\mathrm{S}}\right)^2 \left(1 - c_{\mathrm{A}}^{\mathrm{S}}\right)^2\right] \quad (9)$$

and $c_{\mathrm{A}}^{\mathrm{S}}$ is the equivalent surface fraction of A atoms in B, which is related to the molar atomic volumes:

$$c_{\mathrm{A}}^{\mathrm{S}} = \frac{c_{\mathrm{A}} V_{\mathrm{A}}^{2/3}}{c_{\mathrm{A}} V_{\mathrm{A}}^{2/3} + c_{\mathrm{B}} V_{\mathrm{B}}^{2/3}} \quad (10)$$

Note that $c_{\mathrm{A}}^{\mathrm{S}}$ is not the same as the surface concentration $x_{\mathrm{A}}^{\mathrm{surf}}$.

Miedema's model defines the formation enthalpy as the interface energy of the boundary between Wigner-Seitz atomic cells [33]:

$$\Delta H_{\mathrm{AinB}}^{\mathrm{sol}} = \Delta H_{\mathrm{AinB}}^{\mathrm{interface}} = \frac{V_{\mathrm{A}}^{2/3}}{\left(n_{\mathrm{ws}}^{-1/3}\right)_{\mathrm{av}}}\left[-P\left(\Delta\phi^{*}\right)^2 + Q\left(\Delta n_{\mathrm{ws}}^{1/3}\right)^2\right] \quad (11)$$

where ϕ^* is the chemical potential for electronic charge and n_{ws} is the electron density at the boundary. $\Delta\phi^* = \phi^*_{\mathrm{A}} - \phi^*_{\mathrm{B}}$, $\Delta n_{\mathrm{ws}}^{1/3} = n_{\mathrm{ws\,A}}^{1/3} - n_{\mathrm{ws\,B}}^{1/3}$ and $\left(n_{\mathrm{ws}}^{-1/3}\right)_{\mathrm{av}} = \dfrac{\left(n_{\mathrm{ws}}^{-1/3}\right)_{\mathrm{A}} + \left(n_{\mathrm{ws}}^{-1/3}\right)_{\mathrm{B}}}{2}$. P and Q are empirical constants. In the present research, P=12.35 and Q=9.4P, which are suitable for metals with transition metals. Some literatures use P=10.7 for alloys of monovalent or divalent metals or P=14.2 for alloys of metals with valence>2. These values are also used for calculation, but this changes the result of surface segregation only changed 1-2%. All related parameters are shown in Table 1 [33].

Note that the atomic cell of A will change its volume upon alloying with B, because the chemical surrounding has changed. The volume change depends on the charge transfer at the cell boundaries as given in Eq.(12):

$$\frac{V_A^{2/3}}{\left(V_A^{2/3}\right)_{\mathrm{pure}}} = 1 + \alpha f_B^A \left(\phi_A^* - \phi_B^*\right) \quad (12)$$

where α=0.04 for most of transition metals. α=0.07, 0.10 or 0.14 are also chosen in some literatures. It may change the volume of solute element in alloys by several percent, but the surface segregation is not sensitive to that. Eq.9, 10 and 12 need to be solved together in a self-consistent manner to get the $c_{\mathrm{A}}^{\mathrm{S}}$, $f_{\mathrm{B}}^{\mathrm{A}}$ and $V_A^{2/3}$ of the alloys.

The model has been applied for the enthalpy of solution of hydrides ($\Delta H_{\mathrm{HinA}}^{\mathrm{sol}}$ and $\Delta H_{\mathrm{HinB}}^{\mathrm{sol}}$). Thereby hydrogen should be considered as “metallic” atoms. The transformation of hydrogen from gas to “metallic” atom is accounted for by an extra term ($\Delta H_{\mathrm{trans}}$) in Eq. 12, leading to [34]:

$$\Delta H_{\mathrm{HinM}}^{\mathrm{sol}} = \frac{c_{\mathrm{H}} V_{\mathrm{H}}^{2/3} f_{\mathrm{M}}^{\mathrm{H}}}{\left(n_{\mathrm{ws}}^{-1/3}\right)_{\mathrm{av}}} \left[-P\left(\Delta\phi^*\right)^2 + Q\left(\Delta n_{\mathrm{ws}}^{1/3}\right)^2 \right] + \Delta H_{\mathrm{trans}} \quad (13)$$

where $\Delta H_{\text{trans}} = 100$ kJ/mol. This value is obtained by the combination of the experimental dissociation energy of H_2, theoretical cohesive energy of metallic hydrogen without zero point energy and the reduced value of positive zero point energy [35].

Note that Miedema's model is an approximate method to calculate the mixing enthalpy, that sometimes may deviate from experimental results. The CALPHAD method, provides mixing enthalpy in good agreement with experimental results, but unfortunately only for a limited amount of Pd-alloys. For comparison CALPHAD data for Pd-Ag and Pd-Cu alloys [36, 37], are also used to calculate the surface segregation. The results were used in order to discuss the effect of the mixing enthalpy.

2.3 Langmuir-McLean equation for equilibrium segregation

With all the parameters mentioned above, ΔH_{seg} can be calculated. Then the equilibrium surface concentration of the solute element ($x_{\text{A}}^{\text{surf}}$) can be expressed by the Langmuir-McLean theory for segregation [38]:

$$\frac{x_{\text{A}}^{\text{surf}}}{1-x_{\text{A}}^{\text{surf}}} = \frac{x_{\text{A}}^{\text{bulk}}}{1-x_{\text{A}}^{\text{bulk}}} \exp\left(-\frac{\Delta H_{\text{seg}}}{RT}\right) \quad (14)$$

where T is the absolute temperature at which equilibrium is obtained, if not particularly defined, T is chosen as 600 K as avoid to the two-phase regions in the Pd-alloys with absorbed hydrogen [39]. Clearly, if $\Delta H_{\text{seg}} > 0$, segregation of solute will occur ($x_{\text{A}}^{\text{surf}} > x_{\text{A}}^{\text{bulk}}$), and if $\Delta H_{\text{seg}} < 0$, segregation of solvent will occur ($x_{\text{A}}^{\text{surf}} < x_{\text{A}}^{\text{bulk}}$). The numerical solution is obtained by a self-consistent method using Eq. 14 and Eq. 1-6 for cases (1) to (4).

3. Results

3.1 Surface segregation in vacuum

Surface segregation of Pd alloys in vacuum, is shown by plotting the surface concentration versus the bulk concentration in atom fraction. For the calculations Eq.1 and 3 are used and a

temperature of 600 K is applied. As shown in Fig.2, solute segregation is predicted in Pd-Ag, Pd-Au and Pd-Cu alloys while solvent (Pd) segregation is predicted in Pd-Ni and Pd-Pt alloys on (111) and (100) plane. The difference between the results for the different crystal planes is small and even negligible for Pd-Au and Pd-Ni alloys. All alloys except Pd-Cu maintain an FCC structure over the whole composition range. For Pd-Cu, a wide BCC phase region and two-phase region (BCC-FCC) exist at 600 K [39]. Taking into account this phase transformation, Z_l and Z_v in Eq.1 will be changed. Yet the results reveal that it has little effect on the surface segregation. The result for segregation of all the 40 binaries of composition $Pd_{0.75}A_{0.25}$, at 600 K on the (111) plane, are given in Table 2.

The effect of temperature is shown in Fig.3 for Pd-Ag and Pd-Au on the (111) plane at 298 K, 600 K and 1000 K. Generally, the higher the temperature, the less segregation occurs, because of the increasing entropy contribution to the total energy.

3.2 Surface segregation with adsorption

With gas adsorption on the surface, the adsorption enthalpy should be included (Eq.4). The adsorption energy of H, CO and O on the surface of related metals are listed in Table 3 [27, 40, 41]. The results for surface segregation are shown in Fig.4. Here the adsorbate coverage θ is chosen as 1.

Clearly, surface adsorption has a strong effect on the surface segregation. Moderate segregation of Pd is predicted for Pd-Ag, Pd-Cu and Pd-Ni alloys. However, for Pd-Au and Pd-Pt, complete segregation of Pd is seen almost across the whole composition range. Comparing with the result in vacuum, the segregation of Pd-Ag, Pd-Au and Pd-Cu alloys reversed from solute (A) segregation to Pd segregation. The segregation of Pd in Pd-Pt is further enhanced. This is due to the stronger adsorption energy of H on Pd than on the other metals. Only segregation of Pd-Ni is not changed because the adsorption energy of H is the same for Pd and Ni.

The effect of adsorption of H, CO and O have also been incorporated. Fig.5 shows the surface segregation of Pd-Ag calculated with adsorption of H, CO and O. Comparing with H adsorption, O adsorption slightly enhances the Pd segregation, while the adsorption of CO results in an strong Pd segregation, which is attributed to a much higher adsorption energy of CO on Pd than on Ag. A similar result is also found for Pd-Au. The effect of adsorption mainly depends on the coverage, which may vary with the partial pressure in real applications.

3.3 Surface segregation with absorption

Surface segregation of Pd alloys with hydrogen absorption in the bulk is shown in Fig.6. The amount of hydrogen absorption per metal atom (x_H) is chosen as 0.5. Basically, hydrogen absorption reduces the surface segregation of Pd alloys. In particular, surface segregation of Pd-Ag, Pd-Cu and Pd-Ni is reversed to Pd enrichment, when compared with segregation in vacuum.

Note that 600 K is above the critical temperature for the hydride phase formation for all the Pd alloys discussed here. However, at lower temperature such as 298 K, phase separation may take place for some specific Pd alloys. Taking $Pd_{0.85}Ag_{0.15}$ alloy as an example, at 298 K with x_H=0.5, the alloy will separately consist of metal phase of composition $Pd_{0.85}Ag_{0.15}H_{0.008}$ and hydride phase of composition $Pd_{0.85}Ag_{0.15}H_{0.64}$. Then the surface segregation could be different for the different phases due to the different H/M ratio.

3.4 Surface segregation with adsorption and absorption

Finally, with both hydrogen adsorption (θ=1) on the surface and absorption in the bulk (x_H=0.5), surface segregation of Pd alloys is shown in Fig.7. There is strong Pd segregation for Pd-Au and Pd-Pt alloys, moderate Pd segregation for Pd-Ag and Pd-Au alloys, and slight Ni segregation for Pd-Ni alloy. The results for simultaneous adsorption and absorption of hydrogen in the series of 40 alloys of composition $Pd_{0.75}A_{0.25}$, at 600 K for the (111) plane, are summarised in Table 4.

4. Discussion

4.1 Segregation in vacuum

Literature reporting experimental measurements or theoretical calculations for surface segregation of Pd alloys at various temperatures, is restricted to a selection of binary alloys, [42-52]. Literature results of surface segregation of the 1st atomic layer on (111) plane are summarized in Table 5, to compare with calculations in the present research. Sometimes, the literature results show differences up to 20%. In particular for Pd-Ag alloy, experimental result by scanning tunnelling microscopy (at 920 K) is about 10% higher than the DFT calculation (at 900 K) and 20% higher than the result of broken-bond model. For Pd-Cu alloy, LEISS result (at 700 K) is 10% higher than Kinetic Monte Carlo results and 30% higher than the broken-bond model (at 800 K). And for the LEISS measurement, data at 600 K is lower than that of 700 K, which is theoretically irrational.

In view of the spread in literature data, the model used in the present research qualitatively gives a good prediction of segregating element for all the Pd alloys, *i.e.* solute segregation for Pd-Ag, Pd-Au and Pd-Cu, solvent (Pd) segregation for Pd-Ni and Pd-Pt. As shown in Fig.8, quantitatively the predicted surface fraction of Pd-Au and Pd-Ni is almost the same as experimental results or theoretical calculations by other methods, such as Monte Carlo simulation or density functional theory (DFT) calculation. Generally, the difference between our calculation and literature results is within 10%. However, for Pd-Ag and Pd-Cu, the solute segregation seems underestimated, especially in the Pd-rich region. For Pd-Pt, the Pd segregation is overestimated across the whole composition range. For some data the difference can even be about 20%-30%.

As mentioned above, calculation of mixing enthalpy by Miedema's model may not be always in good agreement with experimental measurements. In order to investigate the effect of mixing enthalpy on the prediction of surface segregation, the CALPHAD method was

applied to Pd-Ag and Pd-Cu alloys. The surface composition upon segregation in vacuum was then calculated. The results were shown in Fig.9. At 600 K, CALPHAD calculation provides qualitatively the same prediction of the surface segregation comparing with the result of Miedema's model, which is reasonable since surface energy is probably the most dominant factor for surface segregation in vacuum. Quantitatively, CALPHAD calculation indicated more Ag segregation, which improved the accuracy of the prediction comparing with literature results shown in Fig.8a. However, both models give almost the same results for Pd-Cu alloys. It can be concluded that mixing enthalpy will not change the predicted segregation tendency, but sometimes might change the prediction of surface composition upon segregation quantitatively in some cases.

Another influencing factor is the short-range ordering (SRO) of the alloys. Recalling that the regular solution model is used to describe the configurational energy in Eq.1, 4, 5 and 6, thereby assuming that for both surface and bulk, the probability of having either A or B, corresponds to that of a random distribution of atoms. However, SRO usually occurs in real alloys, which modifies the probability of nearest neighbours, as well as the segregation enthalpy and entropy. For example, a "Pd cluster" structure has been reported on the surface of Pd-Cu alloy upon segregation at 600 K [49]. In particular, for Pd-Ag and Pd-Cu alloys with negative ω, atoms of the same element tend to form clusters, then the model will underestimate the segregation enthalpy, as well as the surface fraction. While for Pd-Pt alloy with positive ω, the nearest neighbours tend to be of different kind, implying that surface segregation may be overestimated. Only for Pd-Au and Pd-Ni alloys with ω close to zero, the calculation gives quantitatively accurate predictions. A quantitative evaluation for the effect of SRO on segregation was given by M. Polak, et al. [53]. It was shown that the energy contribution of SRO is always negative, therefore SRO tends to increase the solute fraction level at the surface [54]. This is in agreement with the observed difference between the

predicted and experimental results for the alloys in which SRO is expected, Pd-Ag, Pd-Cu and Pd-Pt.

Considering the experimental (or theoretical) uncertainty in the literature data, it can be concluded that our model provides at least a good semi-quantitative prediction of the surface composition upon segregation.

4.2 Effect of elastic strain energy

In general, the size mismatch of a solute atom and a solvent atom leads to a strain field around the solute atom, and a corresponding elastic strain energy. However, previous models usually postulated that this elastic strain energy would be totally eliminated by the atom exchange at the surface [26]. In order to assess the effect of it, surface segregation was calculated both with and without considering the elastic strain energy and the results were compared and discussed.

In Fig.10a, it can be seen that the elastic strain energy indeed has an influence on the surface segregation in vacuum and in gas environment. For Pd-Ag, Pd-Au and Pd-Cu, the composition difference of the topmost atomic layer calculated with and without elastic strain energy is generally about 10%. Due to the comparable elastic modulus and atomic volume, the results are almost the same for Pd-Pt alloy. However, not for Pd-Ni alloy, by adding the elastic strain energy, the surface segregation tendency changes from a slight segregation of Ni to a rather strong segregation of Pd, which is in agreement with literature results as shown in Fig.8d. This is probably because the elastic strain energy of Pd-Ni alloy (14 kJ/mol) is much higher and it also makes a larger contribution to the total segregation enthalpy than that for the other alloys (for example 0.1 kJ/mol for Pd-Pt). On the other hand, with both hydrogen adsorption and absorption (θ=1, x_H=0.5), effect of elastic strain energy seems to be less, as shown in Fig10b. For Pd-Ag, Pd-Cu and Pd-Pt, the difference is less than 10%, while almost the same for Pd-Au and Pd-Pt. Still, for Pd-Ni, the difference is more than 30%. But different

from in vacuum, the segregation tendency is dominated by the gas environment, meaning that the effect of elastic strain energy is hidden by the adsorption energy and formation enthalpy of metal hydrides.

4.3 Effect of gas environment

In vacuum, surface segregation of Pd alloys basically depends on the surface energy of different elements as well as the lateral chemical bonding energy. However, it is quite different in gas environment since the interaction between the gas and alloys, either adsorption on the surface or absorption in the bulk, has a strong impact on the segregation enthalpy. Some surface segregation results of Pd alloys in different gas environments have been reported [55-59]. Adsorption of H involves strong segregation of Pd to the surface for Pd-Ag, Pd-Au and Pd-Pt alloys. For H absorption, there are no results reported since hydrogen has to be adsorbed before it is absorbed. For the case of both H adsorption and absorption, surface segregation of Pd is also observed in Pd-Ag, Pd-Cu and Pd-Pt alloys [60-62]. Qualitatively, the calculations obtained here are all in agreement with these experimental results. For a quantitative comparison, some key parameters such as adsorbate coverage and absorption concentration are needed.

4.4 Effect of co-adsorption

In section 3.2, surface segregation induced by H, O and CO adsorption on the Pd-Ag surface have been predicted separately. However, in real operating conditions of membranes, there will be co-adsorption of H and impurity gases. In these situations, for example co-adsorption of H and CO on the (111) plane of Pd-Ag surface, the segregation enthalpy is similar to Eq.4:

$$\Delta E_{\mathrm{seg}}^{\mathrm{ad+ab}} = \left(\gamma_{\mathrm{A}}\sigma_{\mathrm{A}} - \gamma_{\mathrm{B}}\sigma_{\mathrm{B}}\right) + 2\omega Z_l\left(x_{\mathrm{A}}^{\mathrm{bulk}} - x_{\mathrm{A}}^{\mathrm{surf}}\right) + 2\omega Z_v\left(x_{\mathrm{A}}^{\mathrm{bulk}} - \frac{1}{2}\right) + \theta_{\mathrm{H}}\left(\varepsilon_{\mathrm{AH}} - \varepsilon_{\mathrm{BH}}\right) + \theta_{\mathrm{CO}}\left(\varepsilon_{\mathrm{ACO}} - \varepsilon_{\mathrm{BCO}}\right) \quad (15)$$

Here effects of H and CO adsorption are considered as independent and depend on the corresponding adsorbate coverages θ_H and θ_{CO}.

Co-adsorption of H and CO is a competitive process [49], which means that the total adsorbate coverage of different gases is basically a constant:

$$\Theta \approx \theta_{CO} + \theta_H \quad (16)$$

Assuming that total coverage Θ=1, the value of θ_H and θ_{CO} can simply be changed to reveal the effect of both gases. In Fig.11, the results for surface segregation of Pd-Ag at 600 K with co-adsorption of H and CO are shown. The surface segregation with co-adsorption just gradually varies between the one of adsorption of pure H and CO. However, the relation between the adsorption coverage of different gases may be more complex than simple addition as given in Eq.16.

5. Conclusion

A thermodynamic model has been developed that can predict the surface segregation of binary alloys in vacuum or in a gas environment. Surface composition of Pd alloys upon segregation was predicted by an atom exchange approach. Especially, effect of gas adsorption was considered by the adsorption energy, while gas absorption were accounted for by the formation enthalpy of metal hydrides. Validation through comparison of the calculation and experimental data from available literature shows that the predictions semi-quantitatively agree with experiments. Effect of different factors, such as temperature, surface crystalline orientation, mixing enthalpy, elastic strain energy and short-range ordering, were extensively discussed. The results can be used as a basic guideline to design novel Pd alloys for hydrogen separation membranes or other applications. The model itself offers a convenient and accurate method to predict the surface segregation of not only Pd-based, but also various binary alloys in different gas atmospheres.

Acknowledge

The authors acknowledge the financial support from ADEM, A green Deal in Energy Materials of the Ministry of Economic Affairs of The Netherlands (www.adem-innovationlab.nl). The authors also personally appreciate Mr. Daniel E. Castillo for his help.

Reference

[1] Ruban AV, Skriver HL, Norskov JK. Surface segregation energies in transition-metal alloys. Phys Rev B 1999;59:15990-16000.

[2] Sakurai T, Hashizume T, Jimbo A, Sakai A, Hyodo S. New Result in Surface Segregation of Ni-Cu Binary Alloys. Phys Rev Lett 1985;55:514-517.

[3] Treglia G, Legrand B, Ducastelle F, Saul A, Gallis C, Meunier I, Mottet C, Senhaji A. Alloy surfaces: segregation, reconstruction and phase transitions. Comp Mat Sci 1999;15:196-235.

[4] Brongersma HH, Draxler M, de Ridder M, Bauer P. Surface composition analysis by low-energy ion scattering. Surf Sci Rep 2007;62:63-109.

[5] Lewis FA. Hydrogen in Palladium and Palladium Alloys. Int J Hydrogen Energy 1996;21:461-464.

[6] Tosti S, Basile A, Bettinali L, Borgognoni F, Gallucci F, Rizzello C. Design and process study of Pd membrane reactors. Int J Hydrogen Energy 2008;33:5098-5105.

[7] Adams BD, Chen A. The role of palladium in a hydrogen economy. Mater Today 2011;14:282-289.

[8] World Energy Resources, World Energy Council, 2016.

[9] Dunn S. Hydrogen futures: toward a sustainable energy system. Int J Hydrogen Energy 2002;27:235-264.

[10] Hydrogen Tools, Focusing on Safety Knowledge, https://h2tools.org/.

[11] Ramachandran R, Menon RK. An overview of industrial uses of hydrogen. Int J Hydrogen Energy 1998;23:593-598.

[12] Barelli L, Bidini G, Gallorini F, Servili S. Hydrogen production through sorption-enhanced steam methane reforming and membrane technology: A review. Energy 2008;33:554-570.

[13] Al-Mufachi NA, Rees NV, Steinberger-Wilkens R. Hydrogen selective membranes: A review of palladium-based dense metal membranes. Renew Sust Energ Rev 2015;47:540-551.

[14] Carmo M, Fritz DL, Mergel J, Stolten D. A comprehensive review on PEM water electrolysis. Inter J Hydrogen Energy 2013;38:4901-4934.

[15] Gallucci F, Fernandez E, Corengia P, Annaland M. Recent advances on membranes and membrane reactors for hydrogen production. Chem Eng Sci 2013;92:40-66.

[16] Nenoff TM, Spontak RJ, Aberg CM. Membranes for Hydrogen Purification: An Important Step toward a Hydrogen-Based Economy. MRS Bull 2006;31:735-744.

[17] Adhikari S, Fernando S. Hydrogen Membrane Separation Techniques. Ind Eng Chem Res 2016;45:875-881.

[18] Timofeev NI, Berseneva FN, Makarov VM. New Palladium-based Membrane Alloys for Separation of Gas Mixtures to Generate Ultrapure Hydrogen. Inter J Hydrogen Energy 1994;19:895-898.

[19] Berseneva FN, Timofeev NI, Zakharov AB. Alloys of Palladium with Metals of the Platinum Group as Hydrogen-Permeable Membrane Components at High Temperatures of Gas Separation. Inter J Hydrogen Energy1993;18:15-18.

[20] Yun S, Oyama ST. Correlations in palladium membranes for hydrogen separation: A review. J Membrane Sci 2011;375:28-45.

[21] Braun F, Miller JB, Gellman AJ, Tarditi AM, Fleutot B, Kondratyuk P, Cornaglia LM. PdAgAu alloy with high resistance to corrosion by H2S. Inter J Hydrogen Energy 2012;37:18547-18555.

[22] Tosti S, Bettinali L, Violante V. Rolled thin Pd and Pd-Ag membranes for hydrogen separation and production. Inter J Hydrogen Energy 2000;25:319-325.

[23] Roa F, Way JD, McCormick RL, Paglieri SN. Preparation and characterization of Pd-Cu composite membranes for hydrogen separation. Chem Eng J 2003;93:11-22.

[24] Shu J, Bongondo BEW, Grandjean BPA, Adnot A, Kaliaguine S. Surface segregation of Pd-Ag membranes upon hydrogen permeation. Suf Sci 1993;291:129-138.

[25] Lai T, Lind ML. Heat treatment driven surface segregation in Pd77Ag23 membranes and the effect on hydrogen permeability. Inter J Hydrogen Energy 2015;40:373-382.

[26] Wynblatt P, Ku RC. Surface Energy and Solute Strain Energy Effects in Surface Segregation. Surf Sci 1977;65:511-531.

[27] Tomanek D, Mukherjee S, Kumar V, Bennemann KH. Calculation of Chemisorption and Absorption Induced Surface Segregation. Suf Sci 1982;114:11-22.

[28] Williams PL, Mishin Y, Hamilton JC. An embedded-atom potential for the Cu–Ag system. Modelling Simul Mater Sci Eng 2006;14:817-833.

[29] Christoffersen E, Liu P, Ruban A, Skriver HL, Nørskov JK. Anode Materials for Low-Temperature Fuel Cells: A Density Functional Theory Study. J Catal 2001;199:123-131.

[30] Wynblatt P. Introduction to Interface and Diffusion, Materials Issues for Generation IV Systems, Springer, Dordrecht, 2008, pp. 339-424.

[31] Friedel J. Electronic structure of primary solid solutions in metals. Adv Phys 1954;3:446-507.

[32] Swalin RA. Thermodynamics of Solids, Wiley, New York, 1972.

[33] de Boer FR, Boom R, Mattens WCM, Miedema AR, Niessen AK. Cohesion in Metals, Elsevier, New York, 1988.

[34] Herbst JF. On extending Miedema's model to predict hydrogen content in binary and ternary hydrides. J Alloy Compd 2002;337:99-107.

[35] Bouten PCP, A.R. Miedema AR. On the Heats of Formation of the Binary Hydrides of Transition Metals. J Alloy Compd 1980;71:147-160.

[36] Karakaya I, Thompson WT. The Ag-Pd (Silver-Palladium) System. Bull Alloy Phase Diagr 1988;9:237-243.

[37] Li M, Du Z, Guo C, Li C. A thermodynamic modeling of the Cu–Pd system. CALPHAD 2008;32:439-446.

[38] Hondros ED, Seah MP. The Theory of Grain Boundary Segregation in Terms of Surface Adsorption Analogues. Metall Mater Trans A 1977;8A:1363-1371.

[39] Nayebossadri S, Speight J, Book D. Effects of low Ag additions on the hydrogen permeability of Pd–Cu–Ag hydrogen separation membranes. J Membrane Sci 2014;451:216-225.

[40] Barton DG, Podkolzin SG. Kinetic Study of a Direct Water Synthesis over Silica-Supported Gold Nanoparticles. J Phys Chem B 2005;109:2262-2274.

[41] Nordlander P, Holloway S, Norskov JK. Hydrogen Adsorption on Metal Surfaces. Surf Sci 1984;136:59-81.

[42] Ouannasser S, Eugene J, Dreysse H, Wolverton C, de Fontaine D. Study of surface segregation and order in Ag-Pd alloys. Surf Sci 1994;307-309:826-831.

[43] Wouda PT, Schmid M, Nieuwenhuys BE, Varga P. STM study of the (111) and (100) surfaces of PdAg. Surf Sci 1998;417:292-300.

[44] Ropo M, Kokko K, Vitos L, Kollar J. Segregation at the PdAg(111) surface: Electronic structure calculations. Phys Rev B 2005;71:1-6.

[45] Ropo M, Kokko K, Vitos L, Kollar J, Johansson B. The chemical potential in surface segregation calculations: AgPd alloys. Surf Sci 2006;600:904-913.

[46] Rousset JL, Bertolini JC, Miegge P. Theory of segregation using the equivalent-medium approximation and bond-strength modifications at surfaces: Application to fcc Pd-X alloys. Phys Rev B 1996;53:4947-4957.

[47] Foiles SM. Calculation of the surface segregation of Pd–Cu, Pd–Ag, and Pd–Au alloys. J Vac Sci Technol 1987;5:889-891.

[48] Yi CW, Luo K, Wei T, Goodman DW. The Composition and Structure of Pd-Au Surfaces. J Phys Chem B 2005;109:18535-18540.

[49] Cheng F, He X, Chen Z, Huang Y. Kinetic Monte Carlo simulation of surface segregation in PdeCu alloys. J Alloys Compd 2015;648:1090-1096.

[50] Priyadarshini D, Kondratyuk P, Picard YN, Morreale BD, Gellman AJ, Miller JB. High-Throughput Characterization of Surface Segregation in Cu_xPd_{1-x} Alloys. J Phys Chem. C 2011;115:10155-10163.

[51] Miller JB, Morreale BD, Gellman AJ. The effect of adsorbed sulfur on surface segregation in a polycrystalline Pd70Cu30 alloy. Surf Sci 2008;602:1819-1825.

[52] Helfensteyn S, Luyten J, Feyaerts L, Creemers C. Modelling surface phenomena in Pd-Ni alloys. Appl Surf Sci 2003;212-213:844-849.

[53] Polak M, Rubinovich L. Evaluation of basic surface segregation trends induced by short-range order in solid solutions. Surf Sci 1997;377-379:1019-1022.

[54] Polak M, Rubinovich L. The interplay of surface segregation and atomic order in alloy. Surf Sci Rep 2000;38:127-194.

[55] Ramachandran A, Tucho WM, Mejdell AL, Stange M, Venvik HJ, Walmsley JC, et al. Surface characterization of Pd/Ag23 wt% membranes after different thermal treatments. Appl Surf Sci 2010;256:6121-6132.

[56] Lovvik OM, Opalka SM. Reversed surface segregation in palladium-silver alloys due to hydrogen adsorption. Surf Sci 2008;602:2840-2844.

[57] Noordermeer A, Kok GA, Nieuwenhuys BE. A Comparative Study of the Behaviour of the PdAg(111) and Pd(111) Surfaces Towards the Interaction with Hydrogen and Carbon Monoxide. Surf Sci 1986;165:375-392.

[58] Miller JB, Matranga C, Gellman AJ. Surface segregation in a polycrystalline Pd70Cu30 alloy hydrogen purification membrane. Surf Sci 2008;602:375-382.

[59] Maire G, Hilaire L, Legare P, Gault FG, O'Cinneide A. Auger Electron Spectroscopy Study of Chemisorption-Induced Segregation in a Pd-Au Alloy. J Catal 1976;44:293-299.

[60] Abraham A, Padama B, Kasai H, Budhi YW. Hydrogen absorption and hydrogen-induced reverse segregation in palladium-silver surface. Inter J Hydrogen Energy 2013;38:14715-14724.

[61] Khanra BC, Menon M. Role of adsorption on surface composition of Pd-Cu nanoparticles. Physica B 1999;270:307-312.

[62] Flanagan TB, Park C. Hydrogen-induced rearrangements in Pd-rich alloys. J Alloy Compd 1999;293-295:161-168.

[63] Kiskinova MP, Bliznakov GM. Adsorption and Coadsorption of Carbon Monoxide and Hydrogen on Pd(111). Surf Sci 1982;123:61-76.

Table 1 Basic parameters of related elements. The units of $n_{ws}^{1/3}$ is arbitrary density unit. *K* and *G* represent the bulk modulus and shear modulus, respectively [21].

Element	*V*/ cm^3/mol	ϕ^* / V	$n_{ws}^{1/3}$	γ/ mJ/m^2	*K*/ GPa	*G*/ GPa
Pd	8.89	5.45	1.67	2050	180	44
Ag	10.25	4.35	1.36	1250	100	30
Au	10.19	5.15	1.57	1500	220	27
Cu	7.12	4.45	1.47	1825	140	48
Ni	6.60	5.20	1.75	2450	180	76
Pt	9.10	5.65	1.78	2475	230	61
H	1.69	5.20	1.50	/	/	/

Table 2 Surface segregation of Pd alloys, $Pd_{0.75}A_{0.25}$, in vacuum.
The results are calculated for the (111) plane and at 600K.

Alloy	Segregation element	x_A^{surf} of $Pd_{0.75}A_{0.25}$	Alloy	Segregation element	x_A^{surf} of $Pd_{0.75}A_{0.25}$
Pd-Ag	Ag	0.52	Pd-Na	Na	0.33
Pd-Al	Al	0.37	Pd-Nb	Pd	0.01
Pd-Au	Au	0.71	Pd-Ni	Pd	0.03
Pd-Ba	Pd	0.01	Pd-Pb	Pd	0
Pd-Be	Pd	0	Pd-Pt	Pd	0.01
Pd-Bi	Pd	0	Pd-Re	Pd	0
Pd-Ca	Pd	0.03	Pd-Rh	Pd	0.01
Pd-Cd	Cd	0.56	Pd-Ru	Pd	0
Pd-Co	Pd	0.02	Pd-Sb	Pd	0
Pd-Cr	Pd	0.11	Pd-Sc	Pd	0.06
Pd-Cu	Cu	0.26	Pd-Sn	Pd	0
Pd-Fe	Pd	0.04	Pd-Ta	Pd	0
Pd-Hf	Pd	0.01	Pd-Th	Pd	0
Pd-Ir	Pd	0	Pd-Ti	Pd	0.09
Pd-K	K	0.26	Pd-Tl	Pd	0
Pd-La	Pd	0	Pd-V	Pd	0.08
Pd-Li	Li	0.29	Pd-W	Pd	0
Pd-Mg	Pd	0.17	Pd-Y	Pd	0
Pd-Mn	Mn	0.29	Pd-Zn	Zn	0.54
Pd-Mo	Pd	0	Pd-Zr	Pd	0.02

Table 3 Adsorption energy of H, CO and O on the surface of metals. Unit: kJ/mol [27, 40].

Element	ε_H	ε_{CO}	ε_O
Pd	264	151	377
Ag	229	28	335
Au	211[26]	38	315
Cu	239	63	299
Ni	264	126	377
Pt	239	134	319

Table 4 Surface segregation of Pd alloys, $Pd_{0.75}A_{0.25}$, with both H adsorption and absorption. The results are calculated for the (111) plane and at 600K. Data of adsorption energy of H on metals is obtained by experiments or calculations based on effective medium theory [41].

Alloy	Segregation element	x_A^{surf} of $Pd_{0.75}A_{0.25}$	Alloy	Segregation element	x_A^{surf} of $Pd_{0.75}A_{0.25}$
Pd-Ag	Pd	0	Pd-Ni	Ni	0.40
Pd-Au	Pd	0	Pd-Pt	Pd	0
Pd-Co	Pd	0.03	Pd-Rh	Pd	0
Pd-Cr	Pd	0.10	Pd-Sc	Pd	0
Pd-Cu	Pd	0	Pd-Ta	Pd	0
Pd-Fe	Fe	0.48	Pd-Ti	Pd	0
Pd-Hf	Pd	0	Pd-V	Pd	0
Pd-La	Pd	0	Pd-W	Pd	0
Pd-Mn	Pd	0.11	Pd-Y	Pd	0
Pd-Mo	Pd	0.04	Pd-Zr	Pd	0
Pd-Nb	Pd	0			

Table 5 Surface segregation results of Pd alloys in available literature.
The results are all for the (111) plane.

Ref.	Alloy	T (K)	Method	Segregation (in Ref.)	Segregation (our result)
42	Pd-Ag	1000	Direct configurational averaging method	Ag	Ag
43	Pd-Ag	720 770 820 920	Scanning tunnelling microscopy		
44	Pd-Ag	300 600 800 870 900 1000	Electronic structure calculation		
45	Pd-Ag	600 900	DFT calculation		
46	Pd-Ag	800	Broken-bond model		
47	Pd-Au	773 873	Monte Carlo simulation	Au	Au
46	Pd-Au	800	Broken-bond model		
48	Pd-Au	800	Low energy ion scattering spectroscopy (LEISS)		
49	Pd-Cu	300 500 700 900	Kinetic Monte Carlo simulation	Cu	Cu
50	Pd-Cu	700	Low energy ion scattering spectroscopy (LEISS)		
51	Pd-Cu	600	Low energy ion scattering spectroscopy (LEISS)		
46	Pd-Cu	800	Broken-bond model		
52	Pd-Ni	900	Monte Carlo simulation	Pd	Pd
46	Pd-Ni	800	Broken-bond model		
46	Pd-Pt	800	Broken-bond model	Pd	Pd

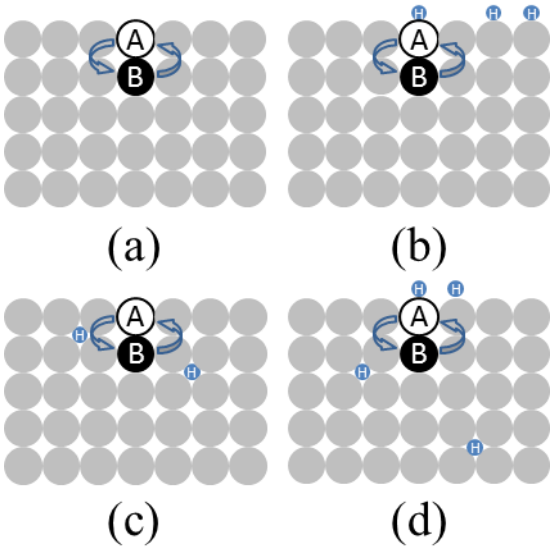

Fig.1 Scheme of surface segregation in terms of the atom exchange model (a) in vacuum; (b) with adsorption; (c) with absorption; (d) with adsorption and absorption.

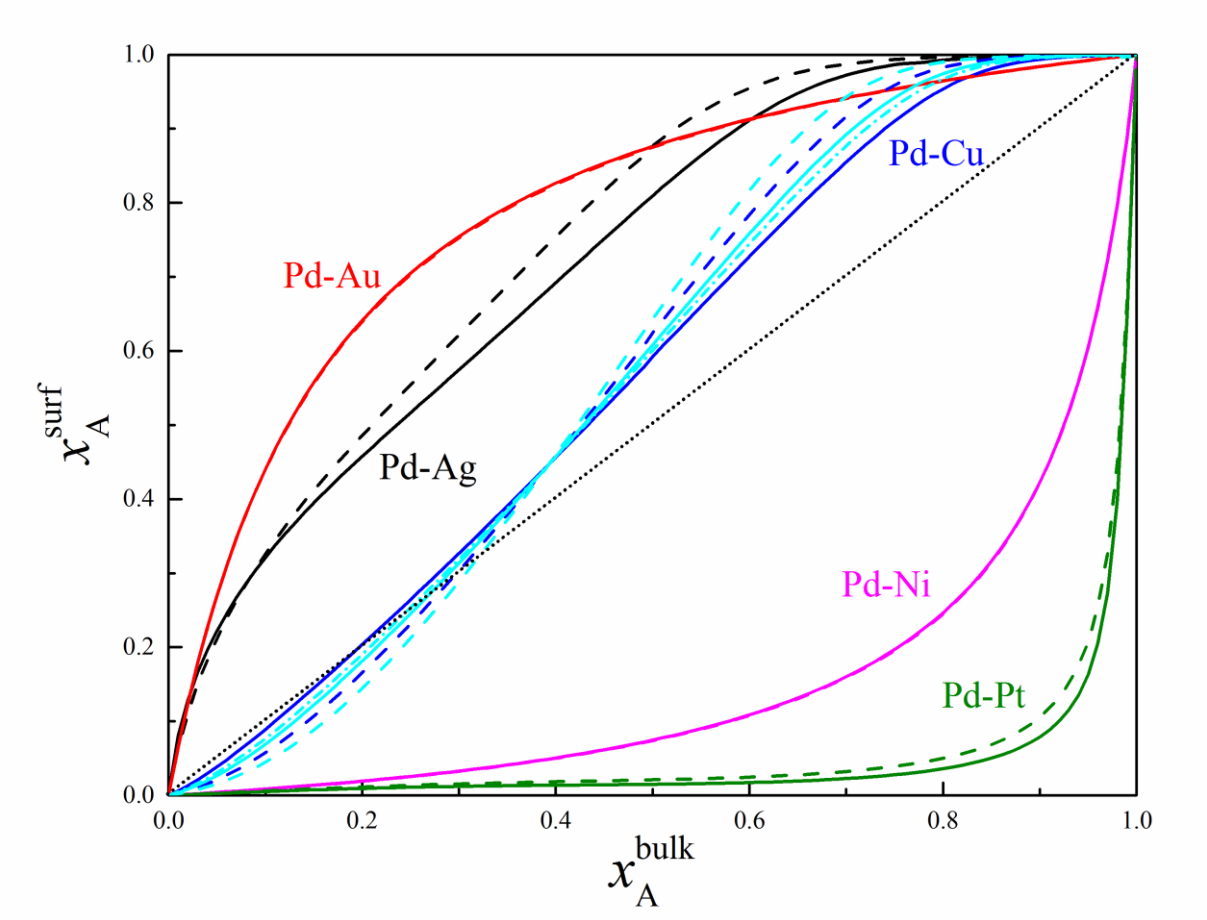

Fig.2 Surface segregation of Pd alloys in vacuum at 600 K.
The solid lines are for (111) plane and dash lines are for (100) planes. Surface segregation of Pd-Cu alloy with BCC structure is shown by light blue lines, solid line for (111) plane, dash line for (100) plane and dash dot line for (110) plane.
The no-segregation line, $x_A^{surf} = x_A^{bulk}$, is indicated by the short-dotted line; above this line the solute segregates, below the line Pd segregates.

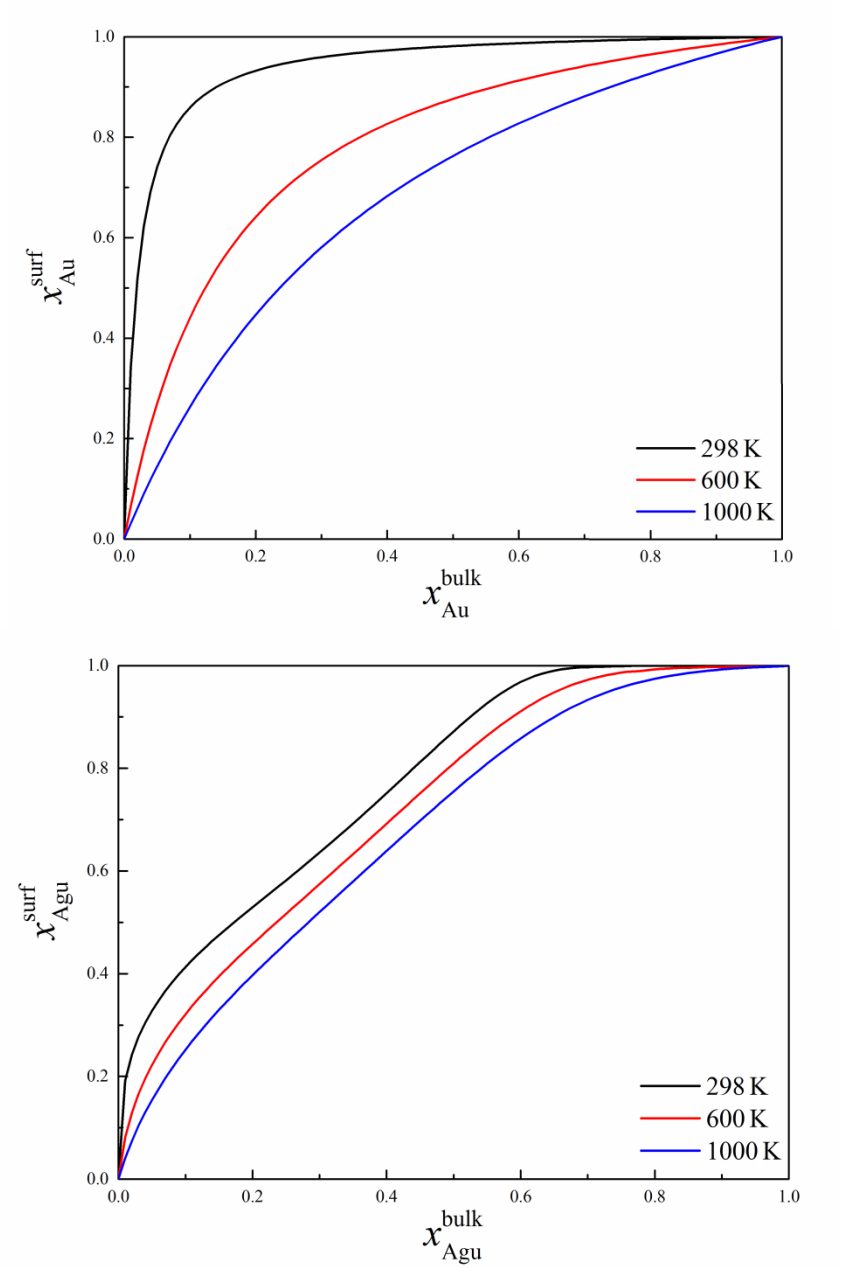

Fig.3 Surface segregation in vacuum at different temperatures: (a) (111) plane of Pd-Ag alloy; (b) (111) plane of Pd-Au alloy.

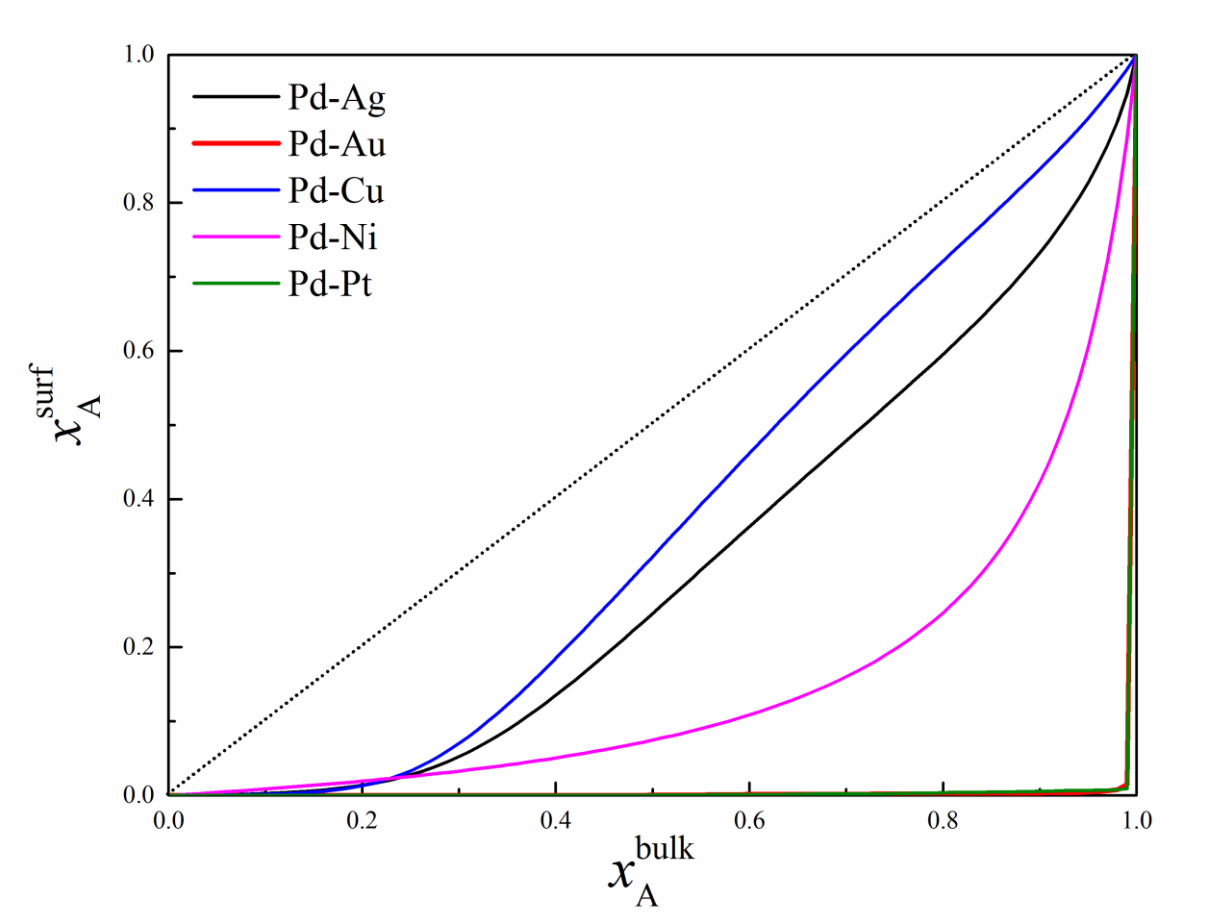

Fig.4 Surface segregation for the (111) plane of Pd alloys with hydrogen adsorption at 600 K. The adsorption coverage θ is chosen as 1. The no-segregation line, $x_A^{surf} = x_A^{bulk}$, is indicated by the short-dotted line; above this line the solute segregates, below the line Pd segregates.

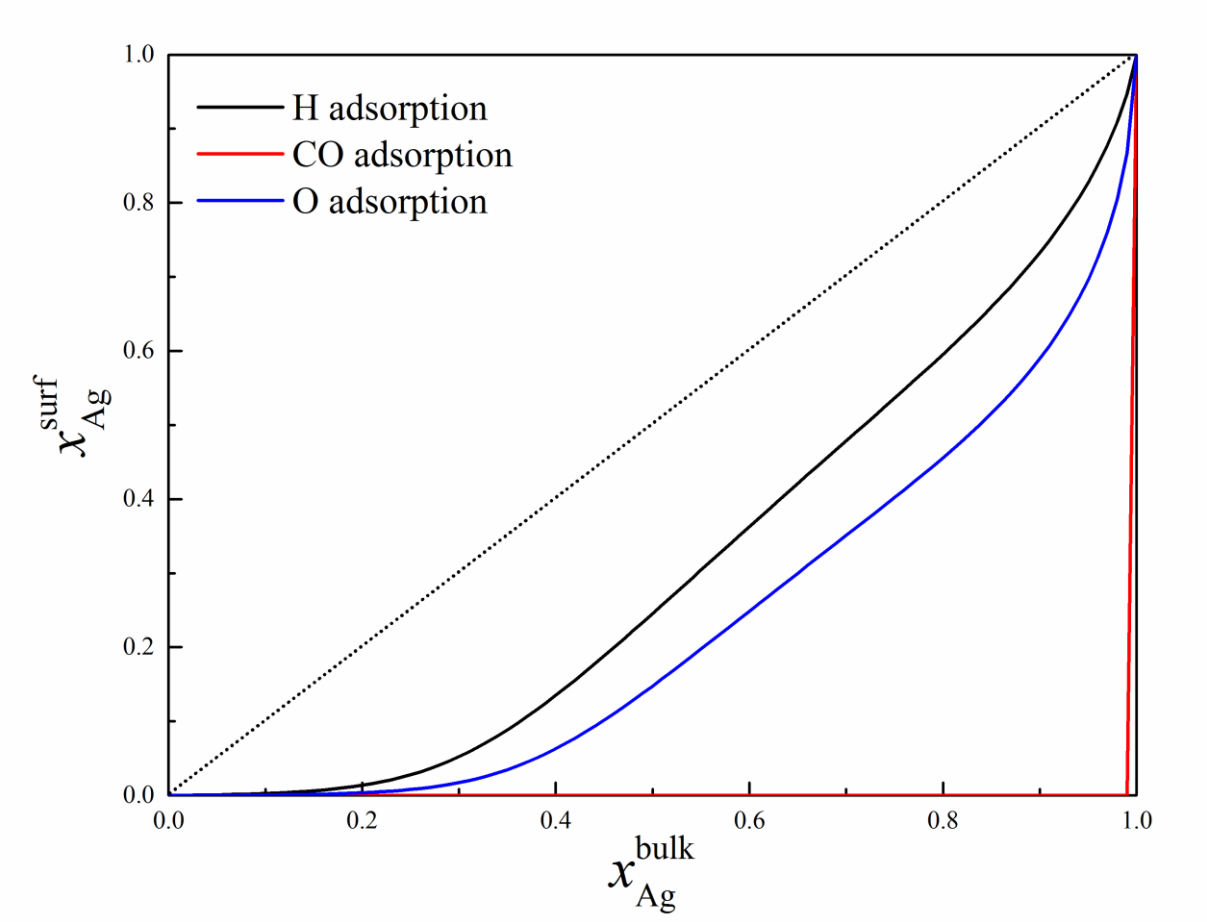

Fig.5 Surface segregation of Pd-Ag alloys with adsorption of different gases at 600 K. The adsorption coverage θ is also chosen as 1. The no-segregation line, $x_A^{surf} = x_A^{bulk}$, is indicated by the short-dotted line; above this line the solute segregates, below the line Pd segregates.

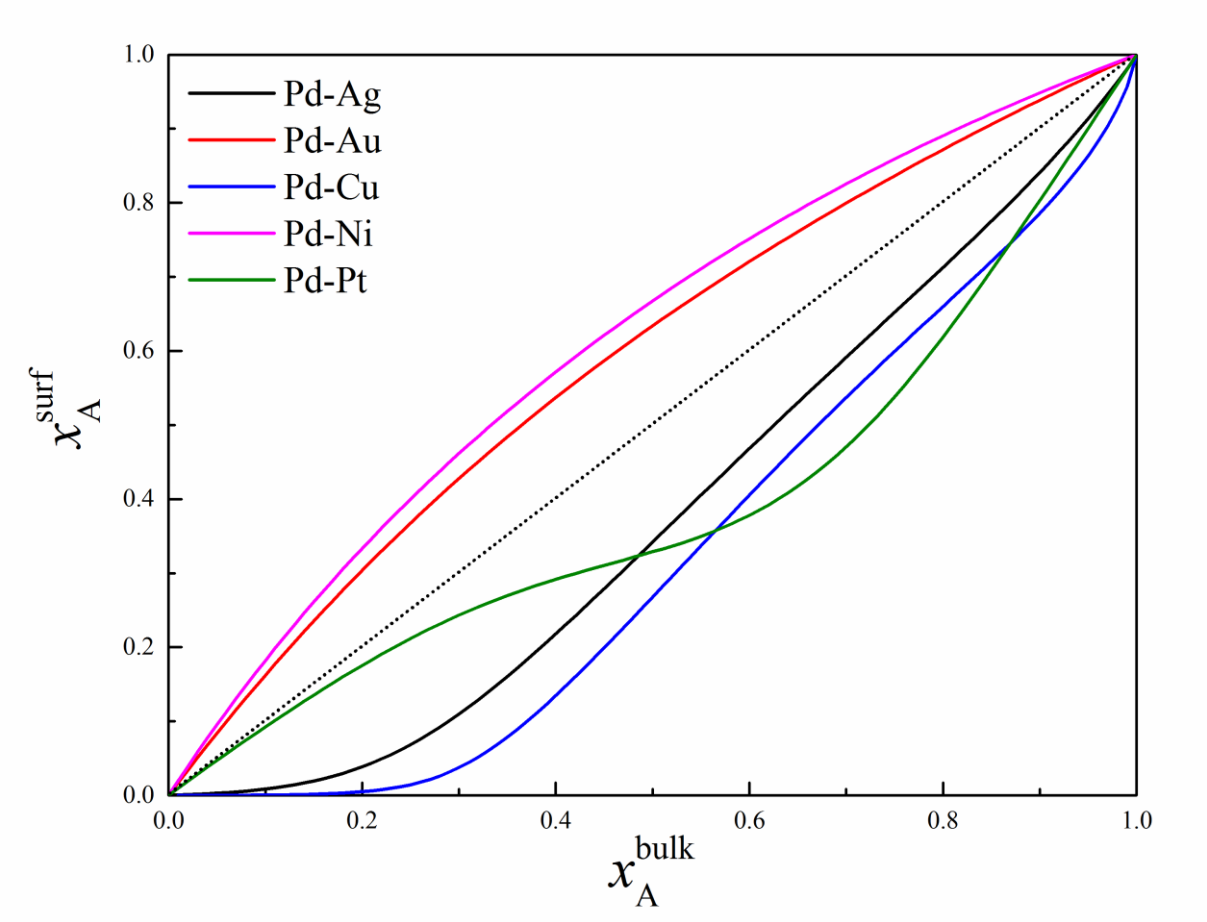

Fig.6 Surface segregation of Pd alloys with hydrogen absorption at 600 K.
The hydrogen concentration x_H is chosen as 0.5. The short-dotted line represents $x_A^{surf} = x_A^{bulk}$.

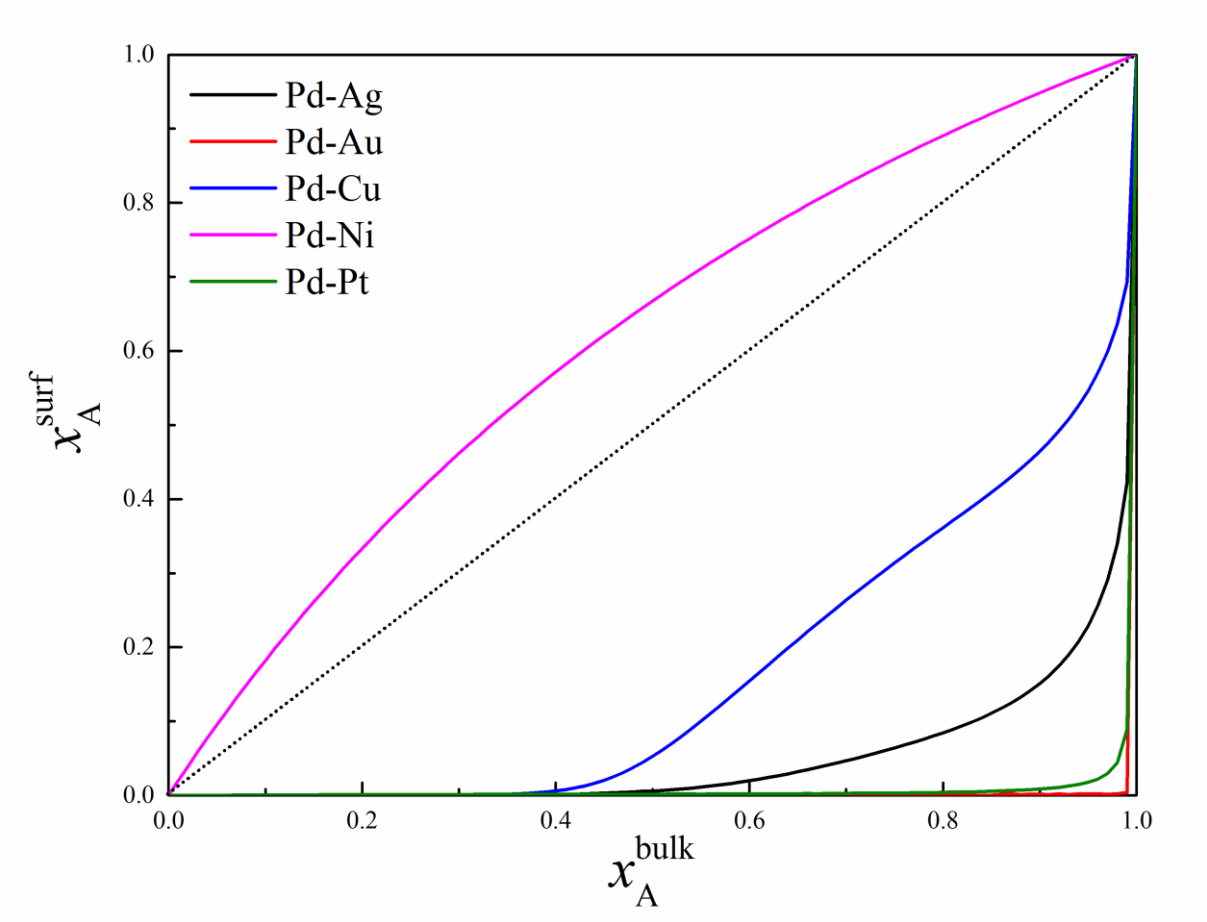

Fig.7 Surface segregation of Pd alloys with both hydrogen adsorption and absorption at 600 K. The adsorption coverage θ is 1 and the hydrogen concentration x_H is 0.5 H/metal. The short-dotted line represents $x_A^{surf} = x_A^{bulk}$.

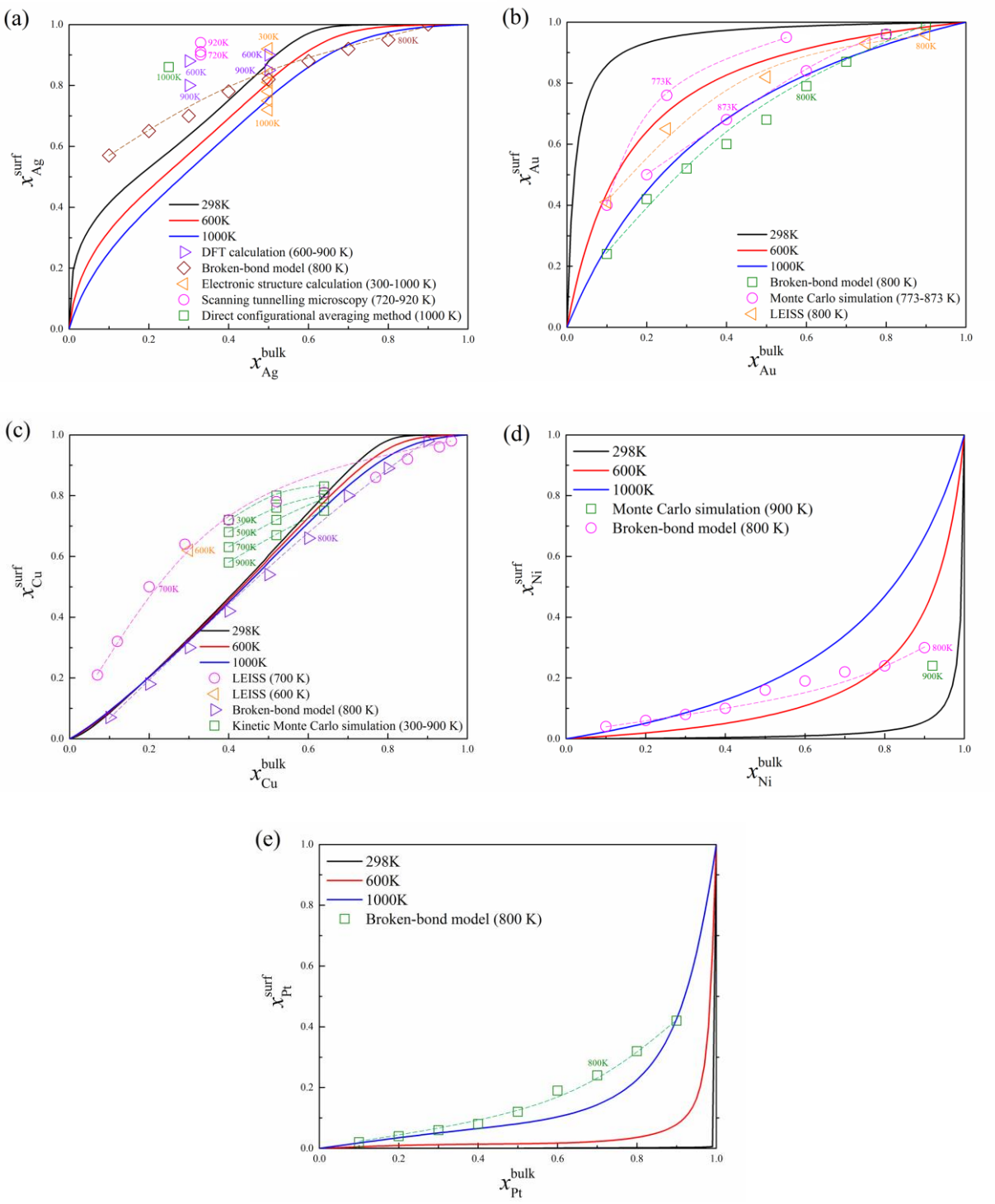

Fig.8 Comparing with results in literature, the calculations using the atom exchange model give a good prediction of surface segregation. (a) Pd-Ag alloy; (b) Pd-Au alloy; (c) Pd-Cu alloy; (d) Pd-Ni alloy; (e) Pd-Pt alloy.

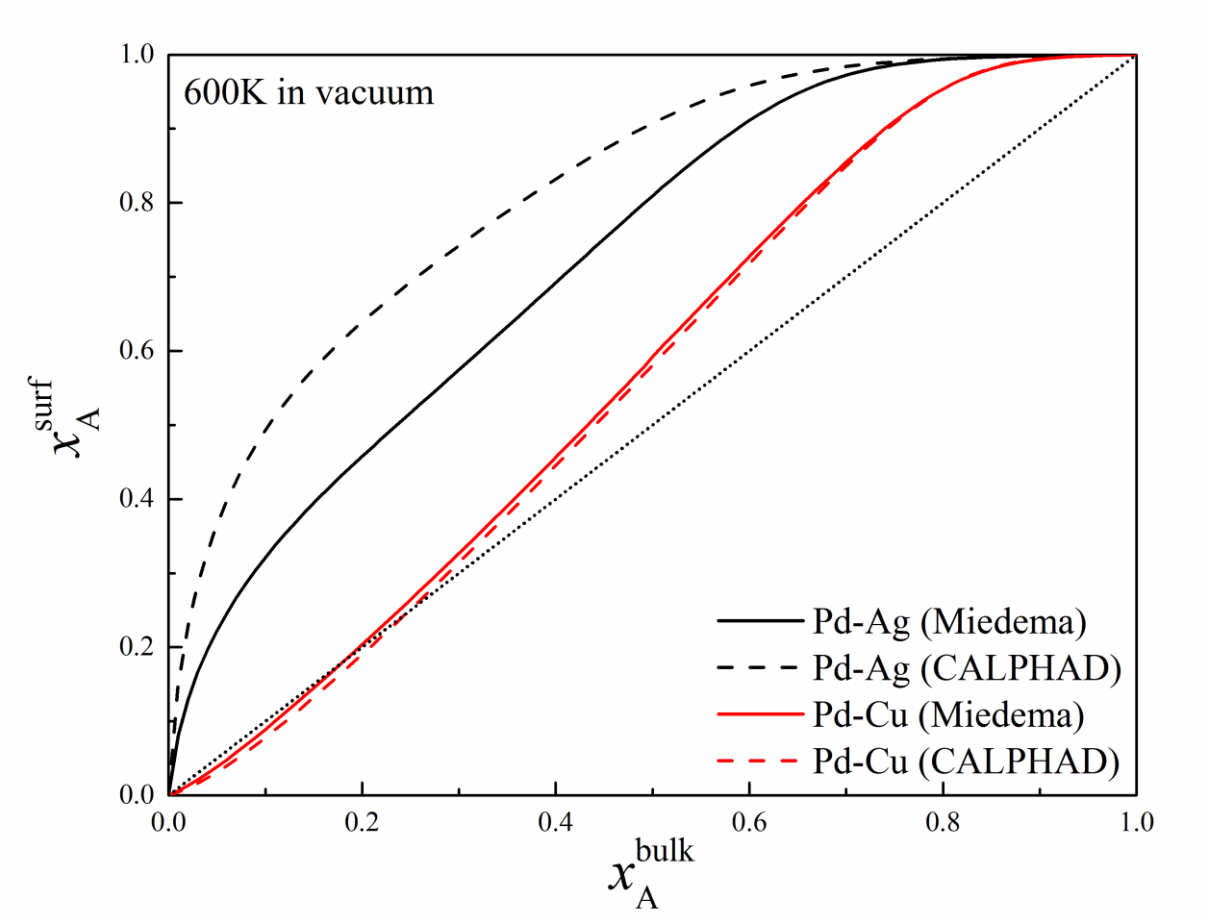

Fig.9 Surface segregation of Pd-Ag and Pd-Cu alloys in vacuum at 600 K. The straight lines are results from Miedema's model and the dash lines are CALPHAD calculation. The short-dotted line represents $x_A^{surf} = x_A^{bulk}$.

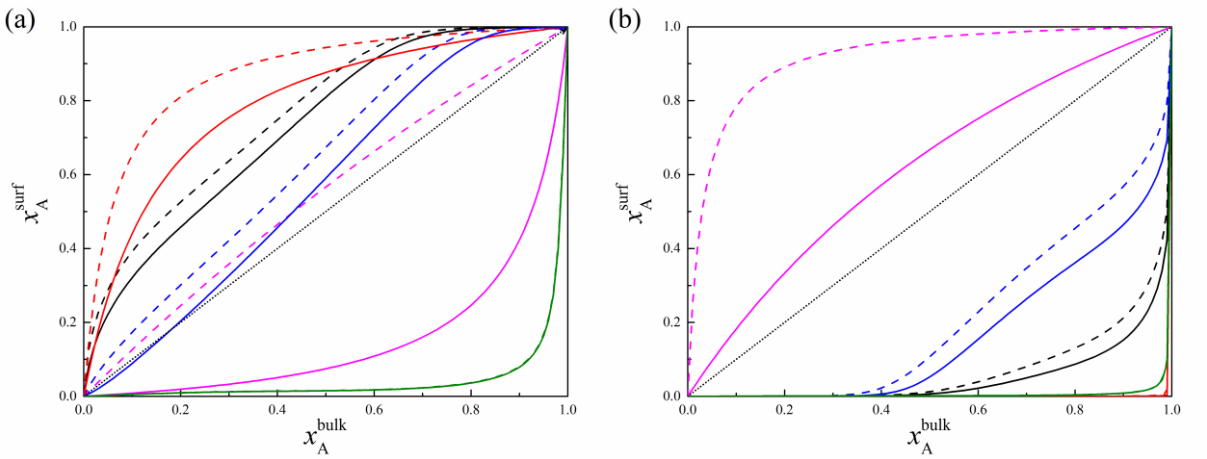

Fig.10 Surface segregation of Pd alloys (a) in vacuum, and (b) with hydrogen adsorption and absorption at 600 K, with and without addition of the elastic strain energy contribution. Lines are: black for Pd-Ag, red for Pd-Au, blue for Pd-Cu, pink for Pd-Ni and green for Pd-Pt. The straight lines are with $\Delta E_{\text{elastic}}$ and dash lines are without. The short-dotted line represents $x_{\text{A}}^{\text{surf}} = x_{\text{A}}^{\text{bulk}}$.

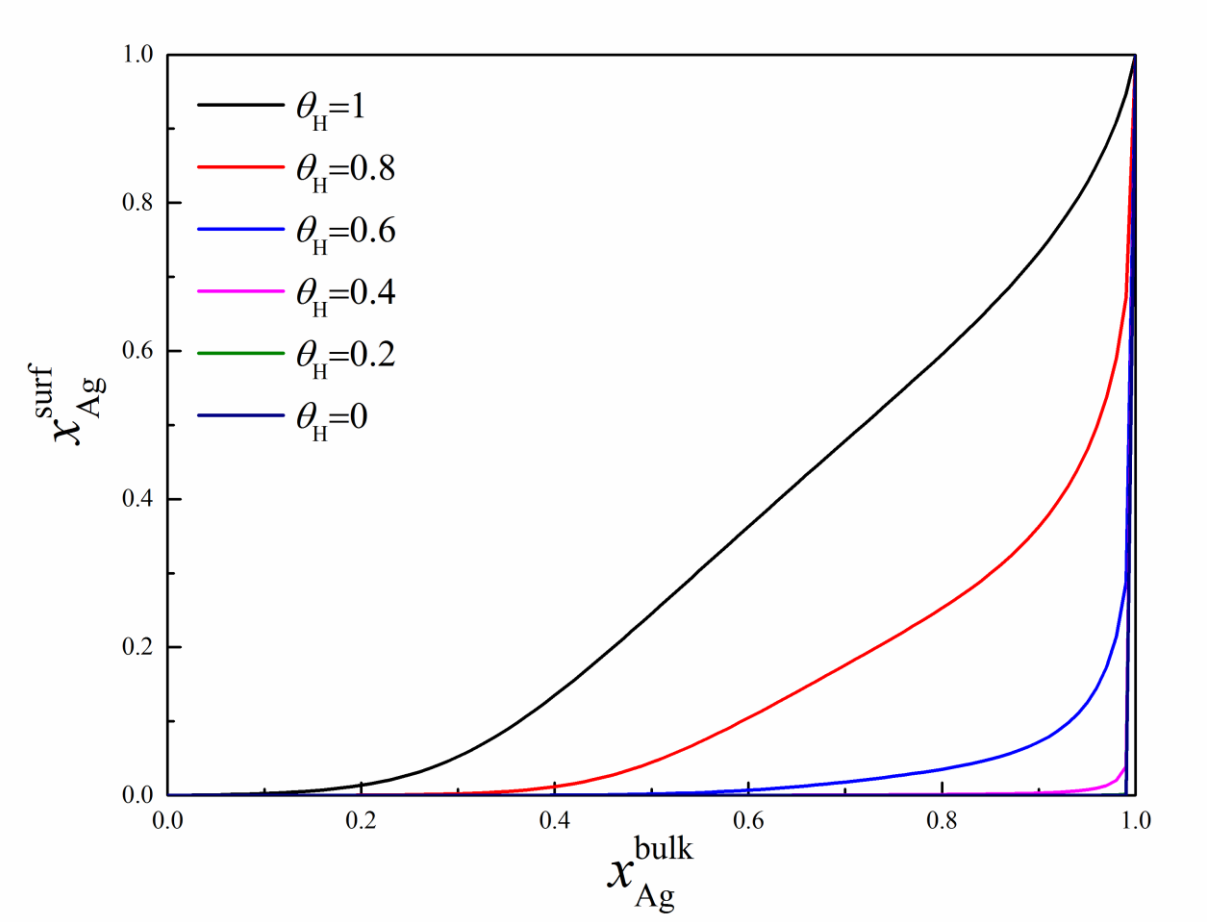

Fig.11 Surface segregation of Pd-Ag alloys with co-adsorption of H and CO at 600 K. The total adsorbate coverage Θ is 1.